National Weather Service
Office of Meteorology

Technical Procedures Bulletin

Subject:

24-h NGM Based Probability and Categorical Forecasts of Thunderstorms and Severe Local Storms for the Contiguous U.S.

Series No. 419

Program Requirements and Development Division, Silver Spring, Md. 20910

SIGNIFICANT CHANGES FROM LAST BULLETIN ON THIS SUBJECT: TPB #281

November 15, 1994
W/OSD21:RMR

This bulletin, written by Ronald M. Reap of the Techniques Development Laboratory, describes the new NGM-Based 24-h probabilistic and categorical forecasts of thunderstorms and severe local storms for the contiguous U.S. that have been operational since late 1994. The probability equations were developed from forecast fields from the National Meteorological Center's (NMC's) Nested Grid Model (NGM), national lightning location data, and severe local storm reports from the National Severe Storm Forecast Center's (NSSFC's) event logs. These equations replaced the limited-area fine-mesh model (LFM) based equations that were operational since the late 1970's. Categorical (yes/no) forecasts of thunderstorms and severe local storms, based on the new NGM-derived forecast probabilities, were also developed to replace the previous LFM versions. The new probabilistic and caterorical forecasts were designed to provide general objective guidance in the 6-60 h timeframe to forecasters at NMC, NSSFC, field forecast offices, and airline terminals.

The new forecasts are valid for the 12-36 h and 36-60 h projections after 0000 UTC and the 6-24 and 24-48 h projections after 1200 UTC. The thunderstorm equations give the unconditional probability of two or more cloud-to-ground lightning flashes occuring in grid blocks that are approximately 48 km on a side. In contrast, the severe local storm equations give the conditional probability of tornadoes, large hail, and/or damaging winds given the occurances of a thunderstorm (defined as the occurance of two or more cloud-to-ground lightning flashes in a grid block).

TPB 281 IS NOW OPERATIONALLY OBSOLETE.

Frederick S. Zbar
Acting Chief, Services Development Branch

24-H NGM-BASED PROBABILITY AND CATEGORICAL FORECASTS OF THUNDERSTORMS AND SEVERE LOCAL STORMS FOR THE CONTIGUOUS U.S.

by Ronald M. Reap, Techniques Development Laboratory

1. INTRODUCTION

This bulletin describes the new NGM-based 24-h probabilistic and categorical forecasts of thunderstorms and severe local storms for the contiguous U.S. that have been operational since late 1994. The probability equations were developed from forecast fields from the National Meteorological Center's (NMC's) Nested Grid Model (NGM) (Hoke et. al. 1989), national lightning location data, and severe local storm reports from the National Severe Storm Forecast Center's (NSSFC's) event logs. These equations replaced the limited-area fine-mesh model (LFM) based equations that were operational since the late 1970's (Reap and Foster 1979). Categorical (yes/no) forecasts of thunderstorms and severe local storms, based on the new NGM-derived forecast probabilities, were also developed to replace the previous LFM versions (Reap et al. 1982; Reap 1983). The new probabilistic and categorical forecasts were designed to provide general objective guidance in the 6-60 h timeframe to forecasters at NMC, NSSFC, field forecast offices, and airline terminals.

The new forecasts are valid for the 12-36 h and 36-60 h projections after 0000 UTC and the 6-24 h and 24-48 h projections after 1200 UTC. The thunderstorm equations give the unconditional probability of two or more cloud-to-ground lightning flashes occurring in grid blocks that are approximately 48 km on a side. In contrast, the severe local storm equations give the conditional probability of tornadoes, large hail, and/or damaging winds given the occurrence of a thunderstorm (defined as the occurrence of two or more cloud-to-ground lightning flashes in a grid block). The categorical forecasts take the form of automated convective outlooks, similar in appearance to the manually-prepared versions from NSSFC, indicating the bounded area(s) where thunderstorms and severe local storms are expected to occur.

2. DEVELOPMENT

a. Method

The thunderstorm forecast equations were derived by applying screening regression techniques and the Model Output Statistics (MOS) approach (Glahn and Lowry 1972) to relate the lightning predictand data to large-scale meteorological predictors obtained from the NGM. Previous evaluations of lightning data from automated networks across the U.S. have clearly revealed the ability of the lightning data to accurately delineate general convective activity (Reap 1986; Reap and MacGorman 1989). The MOS severe local storm forecast equations were similarly derived by relating reports of tornadoes, large hail, and/or damaging winds from the NSSFC event logs to NGM predictors. The automated convective outlooks are prepared following a procedure developed by Reap et al. (1982). Categorical forecasts of thunderstorms and severe local storms are generated from the corresponding MOS probability forecasts and are displayed in a form similar to NSSFC's manually-prepared version.

b. Predictand/Predictor Sample

National lightning location data were obtained for the 1987-90 period from networks operated by the State University of New York at Albany (SUNYA), the National Severe Storms Laboratory (NSSL), and the Bureau of Land Management (BLM). These networks are gated, wideband magnetic direction finding systems that determine the location of flashes to ground by triangulating directions to flashes measured by two or more

stations (Krider et al. 1976). The four-year sample contained approximately 43.6 million cloud-to-ground lightning flashes. The predictand data for severe local storms consisted of reports of tornadoes, large hail (> 3/4"), and/or damaging winds. These reports were extracted from event logs archived and edited at NSSFC to eliminate identifiable sources of error such as redundant, misplotted, or false reports. Following initial processing, the lightning and severe storm reports were related to an 89x113 grid covering the contiguous United States (Fig. 1). Hourly totals for the lightning and severe storm reports were tabulated and stored for each 48-km grid block in the 89x113 array.

The predictor sample included a set of over 100 basic and derived predictors from the NGM. Table 1 shows a listing of the NGM predictors that were offered to the screening regression procedure. Included in Table 1 are a few specialized severe storm indices, i.e., the SWEAT index and total totals index (Miller 1972). Several interactive, or joint, predictor variables, not shown in Table 1, were also offered as potential predictors. Among these are the K stability index (George 1960) multiplied by the 24-h lightning frequency (F) (Reap and Foster 1979); the vertical velocity multiplied by either the K index, the total totals index, or the relative humidity; and the relative humidity multiplied by the K index or total totals index (Bower 1993). The function of the interactive predictors is to at least partially account for the particular, diverse, and probably non- linear combinations of conditions that can lead to the occurrence of the predictand event. In effect, the selected variables are expected to interact with or complement one another in predicting the event. The KF predictor, for example, includes the lightning (thunderstorm) climatology and forces it to be responsive to the daily synoptic situation, as represented by the K stability index. As shown by Reap and Foster (1979) and Charba (1979), the introduction of predictand climatology into the forecast equations results in improved probability forecasts, i.e., variations in predictand climatology are often related to subsynoptic-scale processes, such as land-sea breezes (Reap 1994) and orographic lifting (Reap 1986), that are not adequately resolved by the large-scale model predictors.

c. Unconditional Thunderstorm Probability Equations

Linear screening regression and the MOS approach were used to develop forecast equations that give the unconditional probability of thunderstorms for both the warm (March 15 - September 30) and cool seasons (October 1 - March 14). Forecast equations were developed for each of the four valid periods. The analysis of lightning data and forecast model fields was limited to the 48-km manually-digitized radar (MDR) grid blocks within the CONUS landmass (Fig. 1); no over-water grid blocks were used in the regression analysis.

The resulting forecasts represent the probability of two or more lightning flashes occurring in a 48-km grid block during each of the 24-h valid periods. Forecasts are produced for the 12-36 h and 36-60 h periods following 0000 UTC and the 6-24 h and 24-48 h periods following 1200 UTC. Separate forecast equations were developed for the eastern and western U.S.; the two regions are shown in Fig. 1. Each equation was developed from a generalized dataset created by combining data from all grid blocks in each region. The total sample size for the East was about 2.2 million cases (2949 overland grid blocks times 758 sample days) for the 1987-90 warm seasons. For the West, the warm-season sample size was about 1.3 million cases (1728 blocks times 758 days). For the cool season, the sample size was 1.8 million cases for the East (617 days) and 1.1 million cases for the West (625 days). These represent very large samples which should result in stable forecast equations. Thunderstorm frequency, or the fraction of 48-km grid blocks with two or more flashes to ground, was 18.8% and 13.2% for the East and West, respectively, for the 24-h forecast intervals during the warm season developmental sample. For the cool season, thunderstorm frequency decreased to 3.3% for the East and 0.8% for the West.

Table 2 shows the 12 predictors in the warm-season thunderstorm forecast equations for the East for the 12-36 h and 36-60 h projections after 0000 UTC. Predictors are listed in the order of importance in terms of their contribution to the cumulative reduction of variance. The reduction of variance for the equations in Table 2 was 24.8% (21.4%) with a corresponding multiple correlation coefficient of 0.50 (0.46) for the 12-36 h (36-60 h) projections.

The leading predictor for each projection in Table 2 was the interactive predictor KF formed by combining the climatic lightning frequency F with the K stability index. In daily operation, the climatic frequency is obtained for each day by linear interpolation between monthly mid-point frequency values. Since the KF predictors contain both climatology and a measure of atmospheric stability, they account for most of the general thunderstorm activity and tend to dominate the resulting forecasts. The remaining predictors are normally associated with more localized severe convective thunderstorms and serve to identify such storms in the overall thunderstorm probability forecast. It is interesting to note that another interactive predictor, namely, the 300-mb vertical velocity multiplied by the 300-mb relative humidity (Bower 1993), appears several times in Table 2. This predictor, in effect, identifies regions where potential instability could be released by upward vertical velocity superimposed upon relatively moist air. Predictors selected for the cool season, not shown here, were similar in that the KF term was the leading predictor followed by predictors that captured more localized severe convective weather.

d. Conditional Severe Local Storm Probability Equations

The 24-h equations for severe local storms predict the conditional probability of tornadoes, large hail, and/or damaging winds, given the occurrence of a thunderstorm (two or more cloud-to-ground lightning flashes during the period). Because of the significant decrease in the frequency of severe local storm activity during the summer, separate equations were developed for the spring (March 15 - June 15), summer (June 16 - September 30), and cool (October 1 - March 14) seasons. As in the thunderstorm development, separate equations were developed for the eastern and western U.S. (Fig. 1). Sample spring and summer equations for the 12-36 h projection for the eastern U.S. are shown in Table 3. Predictors are listed in the order of selection, i.e., in order of importance. Sample size, or the number of grid blocks in the 1987-90 spring (summer) samples with thunderstorms (two or more lightning flashes) was 123,619 (265,404) cases for the East. Frequency of occurrence of tornadoes, large hail, or damaging winds for the spring season in the East was 4.4%, dropping by half to 2.2% during summer for the 48-km grid blocks used in the developmental sample. During the cool season, severe local storm frequencies decreased to 1.2% for the East.

Interpreting the results in Table 3 in a general physical sense, we see that maximum conditional probabilities are forecast in regions characterized by strong upper-level winds, a high degree of thermodynamic instability, large wind shears, and favorable low-level cyclonic circulations. In contrast to the KF term in the thunderstorm probability equations, no single term in the severe local storm equations tends to dominate the final probability forecast. Rather, positive contributions from most of the terms in the equations are needed to forecast maximum probability values.

3. Verification

The reliability or bias of the operational thunderstorm equations was evaluated by computing frequencies for 10 thunderstorm probability categories ranging from 0-10% to 90-100%. To compute the frequency for each forecast probability category, the total number of observed grid blocks with two or more lightning flashes to ground in each forecast category was divided by the total number of daily forecasts or grid blocks in that category. The reliability of the warm season thunderstorm probability forecasts for the 12-36 h and 36-60 h projections is shown in Fig. 2. The data points are located at the average forecast probability for each of the ten categories. The number of forecasts (plotted in thousands) is also shown next to each data point. The unlabeled diagonal line represents perfect forecast reliability or zero bias. Fig. 2 indicates that the thunderstorm probability forecasts were highly reliable for the 1989-90 dependent data sample with only a slight tendency to underforecast in the middle ranges. Reliability of the severe local storm probability forecasts for the 12-36 h and 36-60 h projections is shown in Fig. 3. Again, a high degree of reliability and low bias is evidenced by the curves in Fig. 3 for the dependent data sample. Based on our experience with previous MOS thunderstorm and severe local storm forecast equations, no significant degradation is anticipated in the verification statistics for independent data samples.

To further examine the usefulness of the probability forecasts to the operational forecaster, we produced categorical or yes/no forecasts of thunderstorms and severe local storms based on the grid block probabilities. The expected accuracy of such forecasts as a function of various probability threshold values is indicated in Fig. 4 and Fig. 5 for thunderstorms and severe local storms, respectively. The threshold values are, in effect, probability values that could be selected by the forecaster to delineate the regions where thunderstorms or severe local storms are expected to occur. The figures contain several scores suggested by Donaldson et al. (1975). Table 4 shows the contingency table used in computing the scores. The scores computed are the probability of detection (POD), given by $x/(x+y)$, the false alarm ratio (FAR), given by $z/(x+z)$, and the critical success index (CSI), given by $x/(x+y+z)$. For thunderstorm and severe local storm forecasts, it is generally desirable to maximize the POD. The FAR is a generally less useful score, especially for severe local storms, because a significant percentage of the 48-km grid blocks in the region defined by the selected threshold will not contain severe local storm activity, resulting in a consistently high FAR. As a result, a threshold is selected that maximizes the CSI and captures as much of the activity as possible (high POD), and keeps the forecast area as small as possible. The thunderstorm probability forecast in Fig. 6 can be used to illustrate the effect of selecting one of the various probability threshold values shown in Fig. 4. If, for example, a threshold value of 22% is selected, we find that the area defined by this probability isoline would, on average, contain about 80% of the recorded lightning strikes to ground, as shown by the POD in Fig. 4. Referring to Fig. 6, we find that the 22% probability isoline does in fact contain most of the lightning flashes recorded that day. Selection of an appropriate threshold value by the local forecaster is ultimately based on experience gained by using the probability guidance over an extended period of time.

The 22% threshold value in the previous example is one that could be used operationally to delineate regions where thunderstorms are expected to occur. Note, however, that this value is considerably less than the previous value of 35% used as a threshold for thunderstorm probability forecasts from the LFM-based equations (Reap and Foster 1979). An explanation for the significant difference in the threshold values between the NGM-based and LFM-based equations is presented in Section 5.

4. Automated Convective Outlook (AC) Chart

The automated AC's are designed to identify expected areas of thunderstorm activity in addition to more localized regions of severe convective weather (Reap et al. 1982; Reap 1983). The AC's are based on the MOS probability forecasts of thunderstorms and severe local storms. Categorical (yes/no) thunderstorm forecasts are obtained by applying threshold values to the MOS probability forecasts to give bounded areas of thunderstorm activity. The thresholds are obtained from a verification of the probability forecasts, as previously described in Section 3. A similar procedure is used to derive threshold values for producing bounded regions of expected severe local storm activity. In addition, risk codes (APCG, SLGT, MOD, HIGH) are assigned to each bounded area based on the average forecast severe storm probability for the area. The risk codes express the percentage of grid blocks within the severe storm outlook area that are expected to contain severe weather. The automated AC, in effect, provides guidance to NSSFC in the manual preparation of their operational convective outlooks. A sample 12-36 h automated AC chart based on the 0000 UTC forecast cycle for June 10, 1994 is shown in Fig. 7. This particular forecast is from the LFM-based system and is valid for the MDR grid blocks outlined in Fig. 7. The new NGM-based AC chart, currently under development, will not contain the grid block outline shown in Fig. 7 since it covers the entire CONUS.

5. Forecast Implications

Direct statistical comparisons between the new NGM-based thunderstorm and severe local storm probability forecasts and the previous LFM-based probability forecasts (Reap and Foster 1979) are difficult to achieve due to significant differences in the thunderstorm predictand and grid block sizes employed in the developmental samples. The previous LFM development, for example, used MDR data to define thunderstorm occurrences. As shown by Reap and Foster (1979), the relationship between thunderstorms and MDR

data is not exact. Thunderstorm frequencies based on MDR data can, therefore, differ considerably from those based on lightning data which, by definition, indicate the presence of a thunderstorm. Areal coverages provided by radar and lightning networks are also very different, especially in the West where lightning data provide a much better estimation of thunderstorm activity (Reap 1986).*

The grid blocks used in developing the LFM equations were four times as large as those used to develop the NGM-based equations. Grid block size is directly related to predictand frequency and the resulting range of forecast probabilities. Larger grid blocks will automatically result in higher predictand frequencies, a greater range of forecast probabilities, and higher scores for the POD and CSI and lower scores for the FAR. These trends occur since a larger geographical area (and, consequently, a greater percentage of grid blocks) is "verified" by a given thunderstorm occurrence. The NGM-based severe local storm probabilities, for example, range between 0 and 18%, considerably less than the LFM-based probability forecasts which reached maximum values as high as 40%. In effect, lower probabilities from the NGM-based thunderstorm and severe local storm equations are a direct result of the relatively small 48-km grid blocks used in equation development.

The magnitudes of the thunderstorm and severe local storm probability forecasts are, however, not nearly as important as their ability to accurately delineate the potential areas of convective activity. If, for example, we select a threshold value of 6% from Fig. 5 and apply it to the sample severe local storm probability forecast shown in Fig. 8, we find that the area defined by this isoline contains most of the severe local storms that occurred that day, similar to the example for thunderstorms described in Section 3. The area defined by the isoline is also of reasonable size making it useful to the operational forecaster for planning purposes and in preparing severe weather outlooks. In effect, the selection of an appropriate threshold value, based on verification statistics, acts to "scale" the probability forecasts resulting in similar size areas of expected convective activity for the LFM-based and NGM-based outlooks. Threshold values designed to achieve outlook areas similar in size to the LFM-based outlooks and manual outlooks prepared at NSSFC are, in fact, applied daily to NGM-based MOS thunderstorm and severe local storm probability forecasts. The automated convective outlooks derived in this way are used at NSSFC and in the field as guidance in forecasting severe storm activity (Reap et al. 1982; Reap 1983).

In summary, improvements in the performance of the NGM-based MOS products relative to the LFM-based products are anticipated for several reasons. Use of lightning data, for example, has resulted in a greatly improved definition of the thunderstorm predictand, especially over the West where radar data are relatively sparse. The use of lightning data in previous limited MOS developments for the West has led to improved convective weather forecasts in this region (National Weather Service 1987). Use of relatively small (48 km) grid blocks allows the lightning data to more accurately define the local thunderstorm climatology (Reap 1986; Reap and MacGorman 1989; Reap 1994). Improved performance of the NGM relative to the LFM in terms of the movement and positioning of synoptic scale features should also contribute to improved MOS forecasts. Finally, the relatively long 4-year sample of predictor and predictand data results in more stable and accurate forecast equations. As is the case with all MOS forecasts, however, the new NGM-based probability forecasts are highly dependent upon the accuracy of the NGM forecasts used as input. Therefore, the probability guidance may, on occasion, have to be used with caution if the forecaster detects possible errors in the model predictions.

---

*In the development of 6-h and 12-h operational thunderstorm probability equations from the NGM, Bower (1993) also used MDR data along with surface reports and severe local storm data to define thunderstorms in areas approximately 125 km on a side.

6. Graphics Products

The MOS thunderstorm and severe local storm probability forecasts and automated convective outlooks are transmitted twice daily in graphical form over the AFOS communications system and the Family of Services. Product identifiers for the fields (which are the same on AFOS as on the Family of Services AFOS Graphic Service) are listed below:

Probability Forecasts

1200 UTC

NMCGPH02G - 6-24 h unconditional thunderstorm probability
NMCGPH02O - 6-24 h conditional severe local storm probability
NMCGPH03G - 24-48 h unconditional thunderstorm probability
NMCGPH03O - 24-48 h conditional severe local storm probability

0000 UTC

NMCGPH04G - 12-36 h unconditional thunderstorm probability
NMCGPH04O - 12-36 h conditional severe local storm probability
NMCGPH05G - 36-60 h unconditional thunderstorm probability
NMCGPH05O - 36-60 h conditional severe local storm probability

Automated Convective Outlooks

1200 UTC

NMCGPH08G - 6-24 h thunderstorm outlook
NMCGPH08O - 6-24 h severe local storm outlook
NMCGPH09G - 24-48 h thunderstorm outlook
NMCGPH09O - 24-48 h severe local storm outlook

0000 UTC

NMCGPH06G - 12-36 h thunderstorm outlook
NMCGPH06O - 12-36 h severe local storm outlook
NMCGPH07G - 36-60 h thunderstorm outlook
NMCGPH07O - 36-60 h severe local storm outlook

During the period from April 16 to September 15, the 12-36 h thunderstorm and severe local storm probability forecasts from the 0000 UTC forecast cycle also appear on the DIFAX facsimile network in slot D141. They are transmitted once daily at approximately 1303 UTC.

7. References

Bower, J. B., 1993: NGM-based MOS thunderstorm and severe thunderstorm probability forecasts for the contiguous United States. NWS Technical Procedures Bulletin No. 407, NOAA, U.S. Department of Commerce, 16 pp.

Charba, J. P., 1979: Two to six hour severe local storm probabilities: An operational forecasting system. *Mon. Wea. Rev.*, **107**, 268-282.

Donaldson, R. J., Jr., R. M. Dyer, and M. J. Kraus, 1975: An objective evaluator of techniques for predicting severe weather events. *Preprints Ninth Conference Severe Local Storms*, Norman, Amer. Meteor. Soc., 321-326.

George, J. J., 1960: *Weather Forecasting for Aeronautics.* Academic Press, 673 pp.

Glahn, H. R., and D. A. Lowry, 1972: The use of Model Output Statistics (MOS) in objective weather forecasting. *J. Appl. Meteor.*, **11**, 1203-1211.

Hoke, J. E., N. A. Phillips, G. J. Dimego, J. J. Tuccillo, and J. G. Sela, 1989: The regional analysis and forecast system of the National Meteorological Center. *Wea. Forecasting,* **4**, 323-334.

Krider, E. P., R. C. Noggle, and M. A. Uman, 1976: A gated wideband magnetic direction finder for lightning return strokes. *J. Appl. Meteor.*, **15**, 301-306.

Miller, R. C., 1972: Notes on analysis and severe storm forecasting procedures of the Air Force Global Weather Central. Air Weather Service Tech. Rep. 200 (Rev), U.S. Air Force, 102 pp.

National Weather Service, 1987: Verification of the thunderstorm probability equations. NWS Western Region Tech. Attachment No. 87-22, 2 pp. {Available from Techniques Development Laboratory, 1325 East-West Highway, Silver Spring, Md. 20910.}

Reap, R. M., 1994: Analysis and prediction of lightning strike distributions associated with synoptic map types over Florida. *Mon. Wea. Rev.*, **122**, 1698-1715.

____, 1986: Evaluation of cloud-to-ground lightning data from the western United States for the 1983-84 summer seasons. *J. Climate Appl. Meteor.*, **25**, 785-799.

____, 1983: Preliminary evaluation of 1982-83 cool season forecasts from an automated convective outlook (AC) chart. *Preprints 13th Conference Severe Local Storms,* Tulsa, Amer. Meteor. Soc., 47-50.

____, and D. R. MacGorman, 1989: Cloud-to-ground lightning: Climatological characteristics and relationships to model fields, radar observations, and severe local storms. *Mon. Wea. Rev.*, **117**, 518-535.

____, and D. S. Foster, 1979: Automated 12-36 hour probability forecasts of thunderstorms and severe local storms. *J. Appl. Meteor.*, **18**, 1304-1315.

____, ____, and S. J. Weiss, 1982: Development and evaluation of an automated convective outlook (AC) chart. *Preprints 12th Conference Severe Local Storms,* San Antonio, Amer. Meteor. Soc., 110-115.

Table 1. Variables from the NGM offered as predictors to the screening regression analysis.

Predictor (level, if applicable)	
Temperature (1000, 950, 850, 700, 500 mb)	Moisture convergence (950, 850 mb)
Potential temperature (1000, 850, 700, 500, 300 mb)	Wind (speed) shear (950 to 500 mb, 850 to 300 mb, 850 to 500 mb, 700 to 500 mb)
Relative humidity (1000, 950, 850, 700 mb)	Wind divergence (950 mb)
Mean relative humidity (1000 to 500 mb)	Relative vorticity (950 mb)
"u" horizontal wind component (950, 850, 700, 500, 300 mb)	Geostrophic vorticity (500 mb)
"v" horizontal wind component (950, 850, 700, 500, 300 mb)	Vorticity advection (500 mb)
Wind speed (950, 850, 700, 500 mb)	Temperature lapse rate (850 to 500 mb, 850 to 700 mb, 700 to 500 mb)
Sea-level pressure	Height of freezing level
Height (1000, 850, 500 mb)	Wet bulb temperature (850,700 mb)
Total Totals index	Temperature advection (850, 500 mb)
K index	Lifted index (1000, 850 mb)
SWEAT index	Sine day-of-year
Solar altitude	Cosine day-of-year

Table 2. NGM predictors in warm-season thunderstorm probability equations for the eastern U.S. for the 12-36 h and 36-60 h projections following 0000 UTC.

12-36 h	36-60 h
12-36 h K index times 24-h lightning frequency	36-60 h K index times 24-h lightning frequency
950-mb relative vorticity	SWEAT index
300-mb vertical velocity times relative humidity	950-mb moisture convergence
500-mb "u" wind component	300-mb vertical velocity times relative humidity
1000-mb lifted index	850-mb "u" wind component
1000-mb temperature	1000-mb lifted index
300-mb vertical velocity times relative humidity	700-mb vertical velocity times relative humidity
SWEAT index	500-mb "u" wind component
850-mb moisture convergence	850-mb temperature
950-mb moisture convergence	300-mb "v" wind component
Mean relative humidity times K index	300-mb vertical velocity times relative humidity
Cosine day-of-year	500-mb vertical velocity times relative humidity

Table 3. NGM predictors in conditional severe local storm probability equations for the eastern U.S. for the 12-36 h projection following 0000 UTC for the spring and summer seasons.

Spring	Summer
SWEAT index	500-mb wind speed
500-mb "u" wind component	1000-mb lifted index
1000-mb lifted index	Mean relative humidity times total totals index
Mean relative humidity times K index	950-mb relative vorticity
950-mb relative vorticity	500-mb "v" wind component
850-mb lifted index	Solar altitude
Sea-level pressure	850-mb lifted index
700-mb "v" wind component	Sine day-of-year
500-mb vorticity advection	1000-mb relative humidity
950-mb wind speed	850-mb temperature
850-mb height	950-mb to 500-mb wind shear
950-mb temperature	700-mb to 500-mb wind shear

Table 4. Contingency table used in statistical analysis.

	Forecast		
Observed	Lightning	No Lightning	Total
Lightning	x	y	x + y
No Lightning	z	w	z + w
Total	x + z	y + w	x + y + z + w

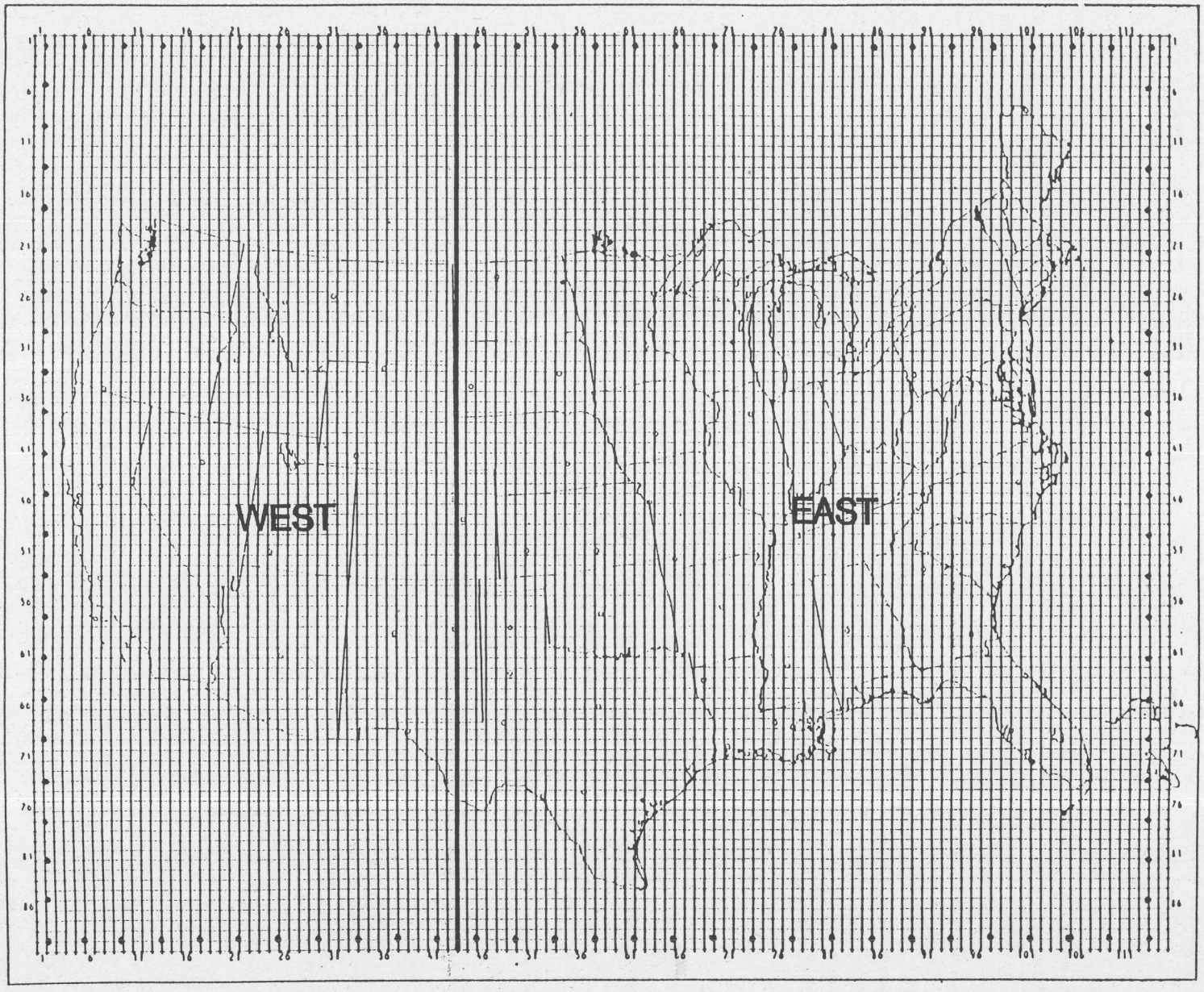

Figure 1. Development grid for MOS thunderstorm and severe local storm equations. Mesh length for 89x113 grid is 48 km at 60 deg north.

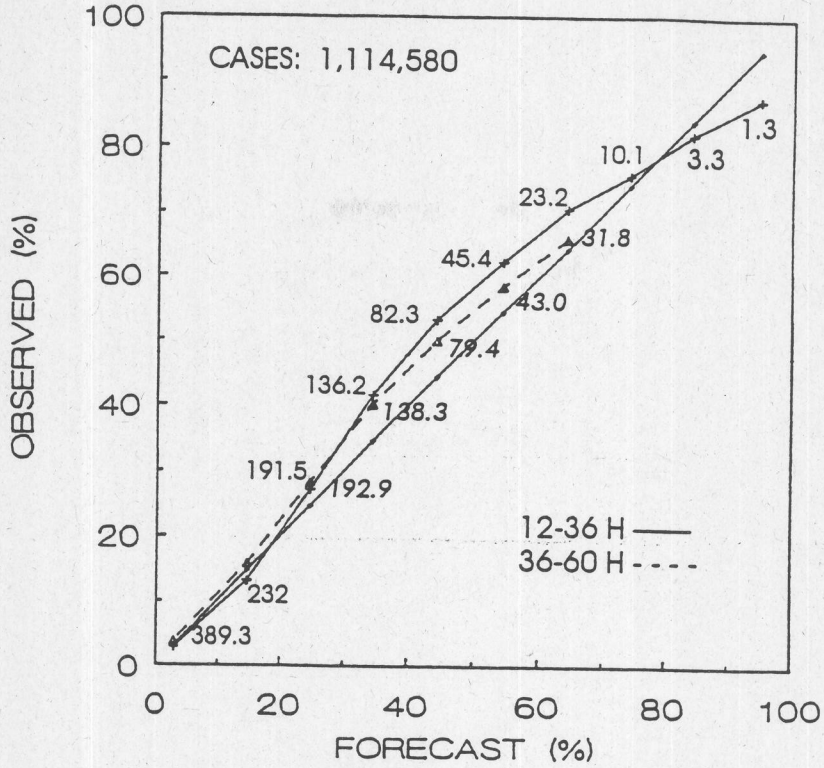

Figure 2. Reliability diagram for MOS thunderstorm probability equations for 12-36 h and 36-60 h projections after 0000 UTC. Forecasts are valid for the March 15 - September 30 warm season periods during 1989-90. Number of cases (thousands) is plotted next to the data points for each probability category.

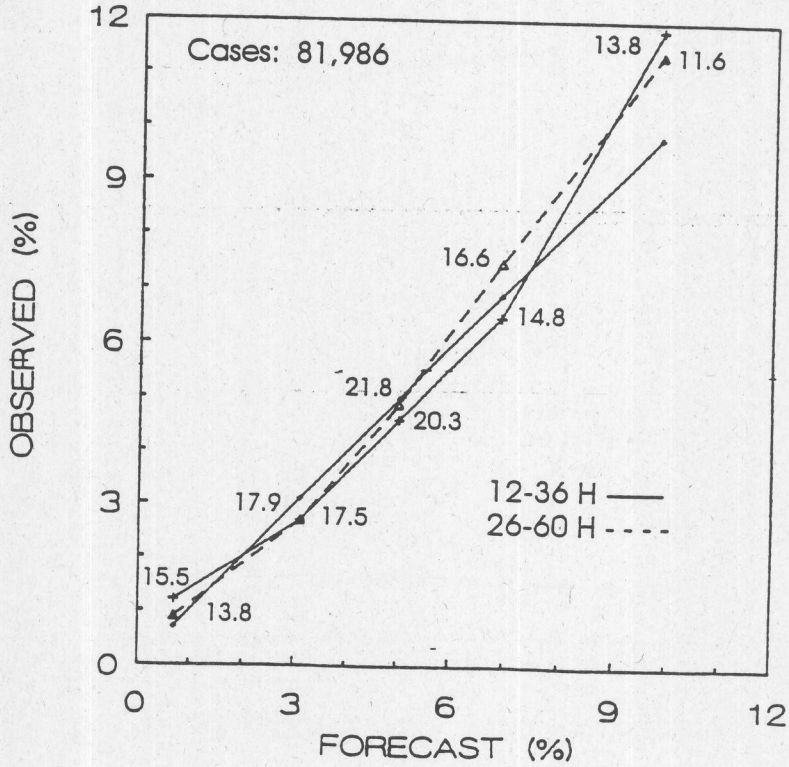

Figure 3. Same as Figure 2 except for MOS severe local storm probability equations.

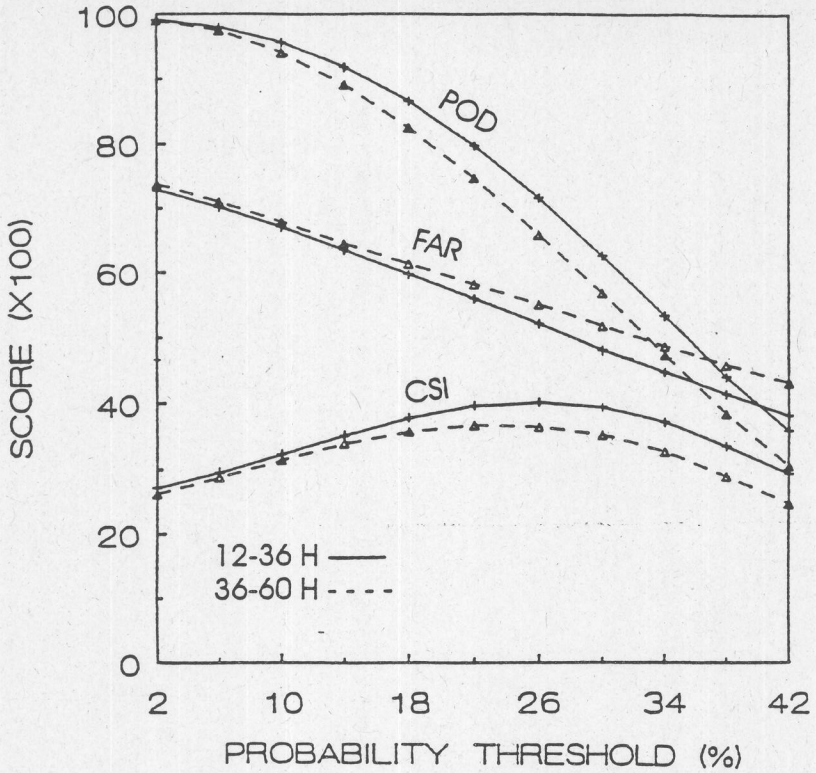

Figure 4. The critical success index (CSI), probability of detection (POD), and false alarm ratio (FAR) for categorical forecasts of thunderstorm occurrence based on various probability thresholds. Forecasts were for 12-36 h and 36-60 h projections after 0000 UTC during 1989-90 warm seasons.

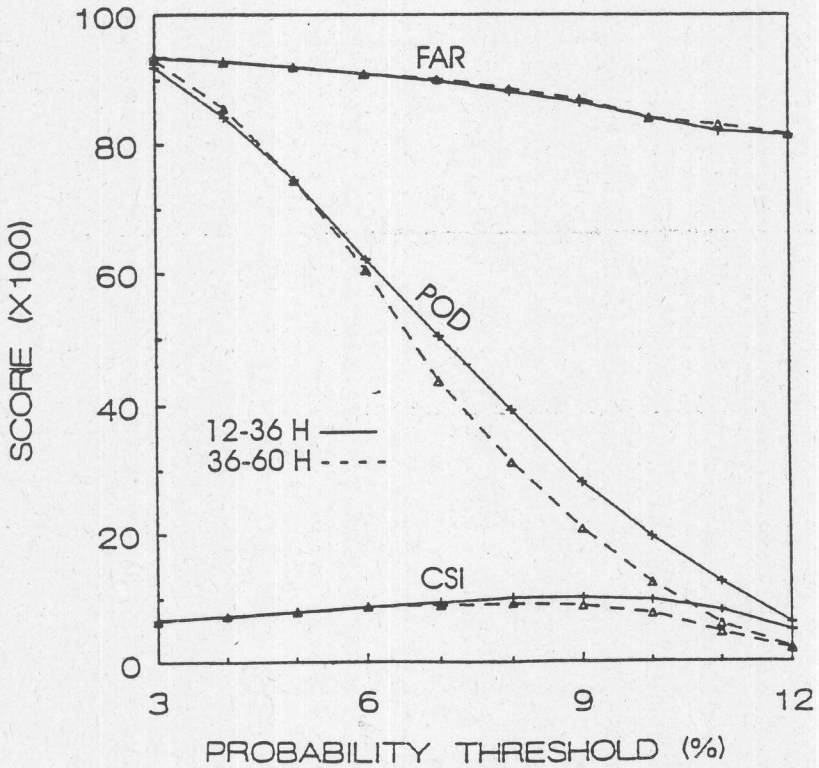

Figure 5. Same as Figure 4 except for MOS severe local storm forecasts during the 1989-90 spring seasons (March 15 - June 15).

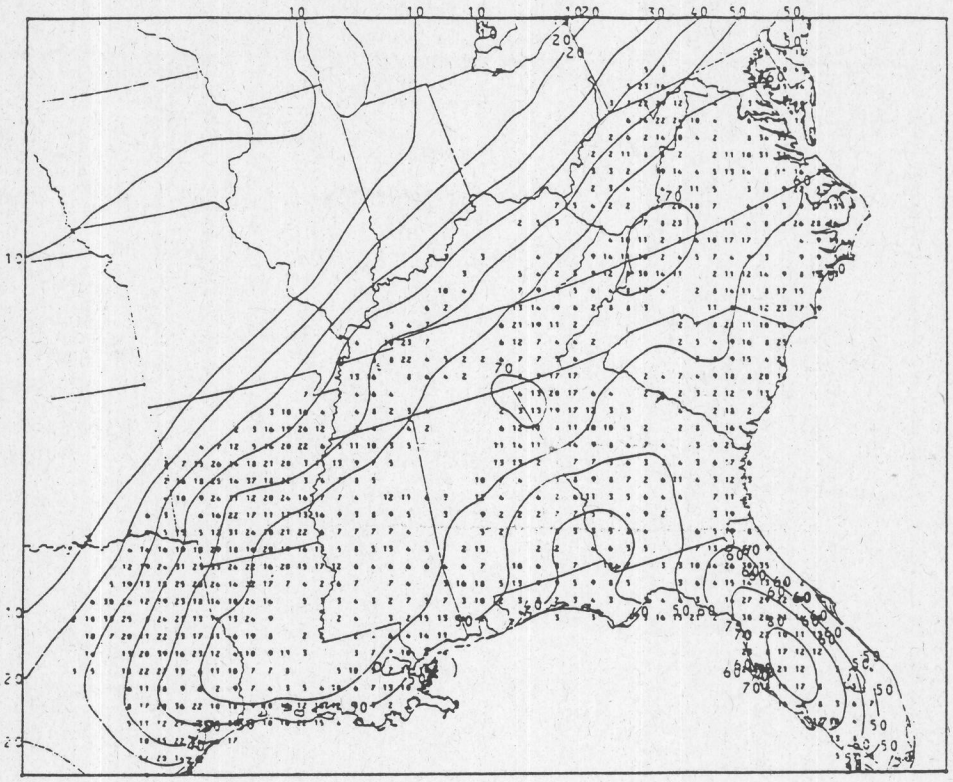

Figure 6. Probability contours of two or more lightning flashes to ground in 48-km grid blocks during 12-36 h projection after 0000 UTC on July 6, 1989. Number of observed flashes is plotted for each grid block.

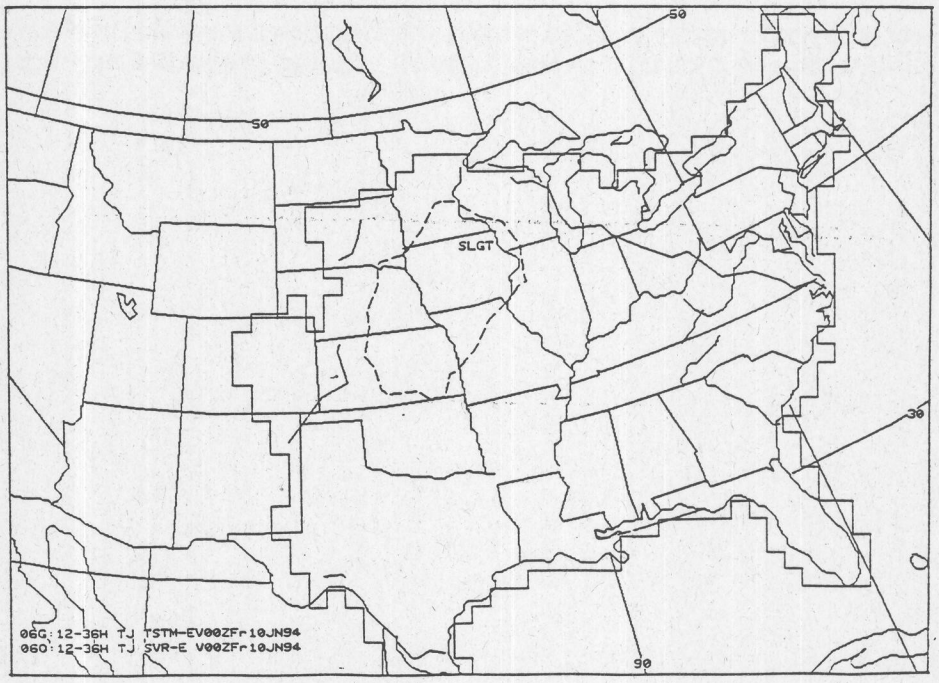

Figure 7. LFM-based automated convective outlook (AC) chart for the 12-36 h period following 0000 UTC on June 10, 1994. Areas of expected thunderstorm (severe local storm) activity are bounded by solid (dashed) lines, respectively. Risk codes (APCG, SLGT, MOD, HIGH) express the percentage of grid blocks within the severe storm outlook area that are expected to contain severe weather.

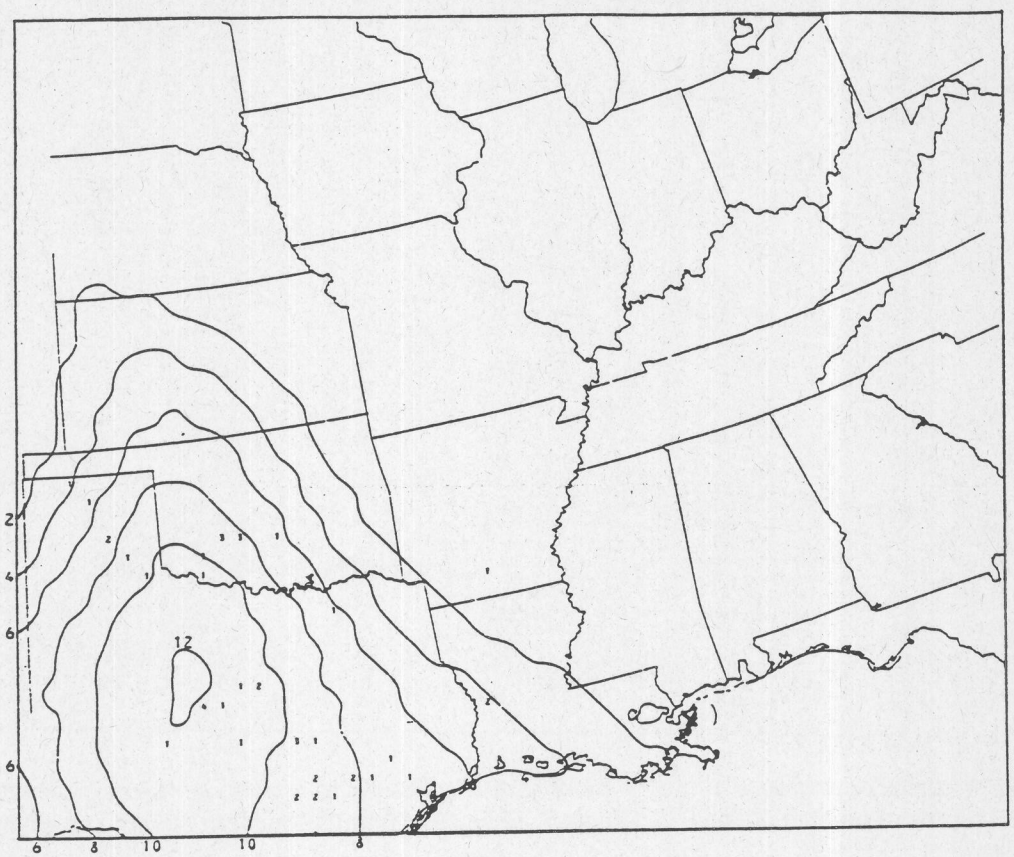

Figure 8. Probability contours of tornadoes, large hail, and/or damaging winds in 48-km grid blocks during 12-36 h projection after 0000 UTC on May 13, 1989. Number of observed severe storms is plotted for each grid block.